

See discussions, stats, and author profiles for this publication at: <https://www.researchgate.net/publication/232905672>

Brønsted/lewis acid synergy in H-ZSM-5 and H-MOR zeolites studied by ^1H and ^{27}Al DQ-MAS solid-state NMR spectroscopy

ARTICLE in THE JOURNAL OF PHYSICAL CHEMISTRY C · NOVEMBER 2011

Impact Factor: 4.77 · DOI: 10.1021/jp203923z

CITATIONS

21

READS

164

7 AUTHORS, INCLUDING:



Zhiwu Yu

Wuhan National High Magnetic Field Center

18 PUBLICATIONS 252 CITATIONS

SEE PROFILE



Shenhui Li

Chinese Academy of Sciences

27 PUBLICATIONS 514 CITATIONS

SEE PROFILE



Anmin Zheng

Chinese Academy of Sciences

104 PUBLICATIONS 1,638 CITATIONS

SEE PROFILE



Jun Xu

Wuhan Institute of Physics and Mathematics

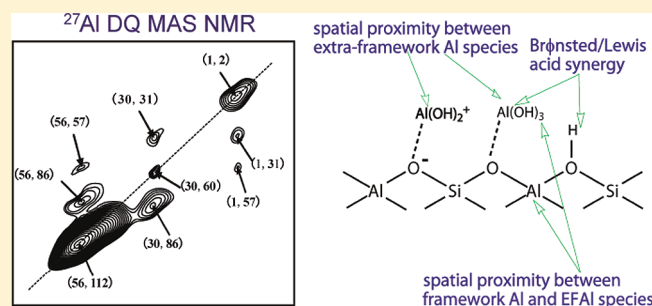
77 PUBLICATIONS 1,399 CITATIONS

SEE PROFILE

Brønsted/Lewis Acid Synergy in H–ZSM-5 and H–MOR Zeolites Studied by ^1H and ^{27}Al DQ-MAS Solid-State NMR SpectroscopyZhiwu Yu,^{†,‡,§} Shenhui Li,^{†,§} Qiang Wang,[†] Anmin Zheng,[†] Xu Jun,[†] Lei Chen,[†] and Feng Deng^{*,†}[†]State Key Laboratory of Magnetic Resonance and Atomic and Molecular Physics, Wuhan Center for Magnetic Resonance, Wuhan Institute of Physics and Mathematics, Chinese Academy of Sciences, Wuhan 430071, China[‡]Graduate School, Chinese Academy of Sciences, Beijing 100029, China

§ Supporting Information

ABSTRACT: The spatial proximities of acid sites in dealuminated H–MOR and H–ZSM-5 zeolites have been comprehensively studied by two-dimensional ^1H and ^{27}Al double-quantum magic-angle spinning (DQ-MAS) NMR spectroscopy. ^1H DQ-MAS NMR revealed the detailed spatial proximities among Brønsted and Lewis acid sites, while ^{27}Al DQ-MAS NMR probed the detailed spatial proximities among various aluminum species in the dealuminated zeolites. It was found that all of the extra-framework aluminum species (EFAL, Lewis acid sites) are always in close proximity to the framework aluminum (Brønsted acid sites) in both H–MOR and H–ZSM-5 zeolites. The result from ^{13}C CP/MAS NMR of adsorbed acetone demonstrated that the spatial proximities between Brønsted and Lewis acid sites lead to a synergy effect that can remarkably enhance the Brønsted acid strength of the dealuminated zeolites. On the basis of these experimental results, we proposed a model to describe the Brønsted/Lewis acid synergy in the dealuminated zeolites.



1. INTRODUCTION

Zeolites are widely used in many acid-catalyzed processes, such as cracking, disproportionation, isomerization, and alkylation reactions in the chemical and petrochemical industry.^{1–6} The acidity properties of zeolites play an important role in all of these processes. In zeolites, Brønsted acid sites are associated with bridging hydroxyl groups (SiOHAl) and four-coordinate framework aluminum, while Lewis acid sites correspond to either extra-framework aluminum (EFAL)⁷ or three-coordinate framework aluminum species.⁸ Many researchers found decades ago that a mild hydrothermal/thermal treatment of various zeolites (such as Y, ZSM-5, MOR, etc.) usually resulted in a partial release of aluminum from zeolite framework and the formation of EFAL species, which considerably improves the catalytic activity of zeolites.^{9–11} Although direct experimental evidence was absent, some of them suggested the Brønsted/Lewis acid synergy (or interaction) to interpret the high catalytic activity of dealuminated zeolites.^{12–17} As such, it is desirable to explore the spatial proximities and interactions among various acid sites to provide the direct experimental evidence for the Brønsted/Lewis acid synergy in dealuminated zeolites.

Solid-state NMR spectroscopy has been widely applied to study the acidity of zeolites.^{18,19} ^1H MAS NMR can give the direct information on various hydroxyl groups, including SiOHAl , AlOH , and SiOH groups, in zeolites.²⁰ In addition, the dynamic properties of Brønsted acidic protons can be investigated by ^1H 2D EXSY NMR method at various temperatures.^{21–29} ^{29}Si MAS NMR can offer

the information about the Si/Al ratio of zeolite framework and the local structure environment around ^{29}Si atoms.²⁷ ^{27}Al single pulse magic angle spinning (MAS) and multiple-quantum (MQ) MAS NMR techniques can be employed to determine the coordination and concentration of both framework Al and EFAL species in zeolites.^{22–24} Moreover, probe molecules, such as $2\text{-}^{13}\text{C}$ -acetone, deuterated pyridine, and trimethylphosphine, were widely used to characterize the acidity of zeolites by using ^{13}C , ^1H , and ^{31}P MAS NMR spectroscopy.^{25–27} However, all of the aforementioned solid-state NMR techniques are unable to provide information about the spatial proximities or interactions between various acid sites in zeolites.

Two-dimensional double quantum magic angle spinning (DQ-MAS) NMR experiment is a useful method for probing spatial proximities or interactions between nuclei in various solid materials, including zeolites.^{28–33} During the past decade, the DQ-MAS NMR technique has been successfully applied not only to spin $I = 1/2$ nuclei, such as ^1H , ^{19}F , ^{29}Si , ^{31}P , but also to quadrupolar nuclei system, such as ^{27}Al and ^{23}Na . On the basis of ^1H DQ-MAS NMR and ^{13}C MAS NMR of adsorbed $2\text{-}^{13}\text{C}$ -acetone, we obtained²⁸ the detailed spatial proximities between Brønsted and Lewis acid sites in dealuminated H–Y zeolite and demonstrated that the spatial proximities could result in a

Received: April 27, 2011

Revised: October 7, 2011

Published: October 07, 2011

synergy effect, which remarkably increases the acid strength of the zeolite. More recently,²⁹ by employing ²⁷Al DQ-MAS NMR spectroscopy, we revealed the detailed spatial proximities among various aluminum species in dealuminated H–Y zeolites.

As a continuous work, in this contribution, to examine whether the Brønsted/Lewis acid synergy effect is also present in other industrially important zeolites, we explored the spatial proximities of Brønsted and Lewis acid sites in H–ZSM-5 and H–MOR zeolites by means of two-dimensional ¹H and ²⁷Al DQ-MAS NMR techniques in conjunction with one-dimensional ¹H, ²⁷Al, and ²⁹Si MAS NMR spectroscopy. The Brønsted/Lewis acid synergy effect on the acid strength of the dealuminated H–ZSM-5 and H–MOR zeolites was also confirmed by ¹³C CP/MAS NMR of adsorbed 2-¹³C-acetone.

2. EXPERIMENTAL SECTION

2.1. Sample Preparation. Powdered, binderless Na–ZSM-5 and Na–MOR zeolites were purchased from the Catalyst Co. from Nankai University, Tianjin, People's Republic of China. Both the Na–ZSM-5 and the Na–MOR zeolites were exchanged in 1 mol/L aqueous solution of NH₄NO₃ at 353 K for 6 h and then washed with distilled water. The process was repeated four times. Subsequently, the resultant NH₄–ZSM-5 and NH₄–MOR zeolites were dried in air at 353 K overnight. To prepare nondealuminated H–ZSM-5 and H–MOR zeolites, the obtained NH₄–ZSM-5 and NH₄–MOR samples were deaminated and dehydrated on a vacuum line (<10^{−5} Torr).²⁸ Dealuminated H–ZSM-5 and H–MOR zeolites were prepared as follows: the NH₄–ZSM-5 and NH₄–MOR zeolites were packed in a shallow bed configuration on a quartz crucible and then calcined at 873 K for 5 h in air. The heating temperature was raised from room temperature to a target temperature at a rate of 5 K/min. The calcined samples as mentioned above are denoted hereafter as H–MOR-600 and H–ZSM-600. The Si/Al ratios determined by ICP-AES chemical analysis are 12.8 and 4.3 for parent H–ZSM-5 and H–MOR zeolites, respectively.

2.2. Solid-State NMR Experiments. ¹H, ²⁹Si, and ¹³C MAS NMR experiments were performed on a Varian Infinity-plus 400 spectrometer at a resonance frequency of 400.1, 79.5, and 100.6 MHz, respectively. Prior to each ¹H MAS and ¹H DQ-MAS NMR experiment, ca. 0.2 g of the sample was packed into a glass tube, which was later connected to a vacuum line. The temperature was gradually increased at a rate of 1.5 K/min, and kept at 673 K at the pressure below 10^{−5} Torr for 12 h to dehydrate the samples. After the samples were cooled to room temperature, the glass tubes were flame-sealed. Next, the sealed samples were transferred into a 4 mm NMR rotor (tightly sealed by a Kel-F cap) under a dry nitrogen atmosphere in a glovebox. ¹H MAS NMR spectra were acquired with a $\pi/2$ pulse length of 2.65 μ s, a spinning rate of 15 kHz, and a recycle delay of 5 s. ¹H DQ-MAS NMR experiments were carried out on a 4 mm probe with a sample spinning rate of 13.477 kHz, and the DQ coherences were excited and reconverted with the POST-C7 pulse sequence.³⁴ The increment interval in the indirect dimension was set to 20 μ s, and 128 t_1 increments and 256 scans accumulations for each t_1 increment were used in the ¹H DQ-MAS NMR experiments. ²⁹Si MAS NMR spectra with high-power proton decoupling were recorded on a 7.5 mm probe with a spinning rate of 5 kHz, a $\pi/4$ pulse length of 2.6 μ s, and a recycle delay of 80 s. ¹³C CP/MAS NMR of adsorbed acetone was used to characterize the acid strength of H–ZSM-5 and H–MOR zeolites. Prior to the ¹³C

CP/MAS NMR experiment, a controlled amount of ¹³C isotope-enriched 2-¹³C-acetone was introduced and frozen into dehydrated zeolites by liquid N₂. Finally, the sample was transferred into the NMR rotor under a dry N₂ atmosphere in a glovebox. Typically, the ¹H→¹³C CP/MAS NMR experiments were performed on a 5 mm probe with a contact time of 5 ms, a recycle delay of 4 s, and a sample spinning rate of 7 kHz. ²⁷Al MAS and ²⁷Al DQ-MAS NMR experiments were carried out on a Bruker AVANCE III 800 spectrometer at a resonance frequency of 208.6 MHz using a 3.2 mm HXY triple-resonance MAS probe at a sample spinning rate of 21.5 kHz. ²⁷Al MAS NMR spectra were recorded by small-flip angle technique with a pulse length of 0.5 μ s (< $\pi/12$) and a recycle delay of 1 s. A CT-selective $\pi/2$ pulse 19 μ s and π pulse 38 μ s were used for the ²⁷Al DQ-MAS experiments, and the signal sensitivity was enhanced by initiating each transient by the FAM scheme.³⁵ DQ coherences were excited and reconverted using the BR2₁ pulse sequence³⁶ with $\tau_{\text{exc}} = \tau_{\text{rec}} = 1116.30 \mu\text{s}$, following the general scheme of 2D multiple-quantum spectroscopy of dipolar-coupled quadrupolar spins. The rotor-synchronized increment interval in the indirect dimension was set to 46.51 μ s, and the two-dimensional data sets consisted of 30 $t_1 \times 400 t_2$ points. 12 800, 14 080, 10 240, and 13 056 FIDs were acquired for each t_1 increment using a recycle delay of 0.4 s, for obtaining the 2D ²⁷Al DQ spectrum of parent H–ZSM-5, dealuminated H–ZSM-5, parent H–MOR, and dealuminated H–MOR, respectively. The chemical shifts of ¹H, ¹³C, and ²⁹Si were referenced to TMS, while that of ²⁷Al was referenced to 1 mol/L aqueous Al(NO₃)₃.

3. RESULTS AND DISCUSSION

3.1. Effects of Calcination. Figure 1 shows the ¹H, ²⁷Al, and ²⁹Si MAS NMR spectra of H–ZSM-5 and H–MOR zeolites before and after the calcination treatments. For parent H–ZSM-5 zeolite, only two main resonance peaks at 4.4 and 2.2 ppm were observed (Figure 1a), which can be attributed to bridging SiOHAl groups (Brønsted acid sites) and nonacidic SiOH, respectively.³⁷ Calcination of the sample results in a new resonance peak at 2.9 ppm in the ¹H MAS spectra of H–ZSM-5–600 sample, which can be assigned to extra-framework AlOH species (Lewis acid sites).³⁸ The ¹H MAS NMR spectra of parent and dealuminated H–MOR zeolites are similar to those of H–ZSM-5 zeolites. The signals at 4.3, 2.8, and 2.0 ppm are ascribed to the bridging SiOHAl groups, the extra-framework AlOH species, and the nonacidic silanols, respectively. The integrated peak areas obtained from spectral deconvolution are summarized in Table 1. It is noted that, after calcinations treatment of the samples, notable decreases in the signal intensities of Brønsted acidic protons in both H–ZSM-5 (4.4 ppm) and H–MOR (4.3 ppm) zeolites were observed, indicating that the framework Al atoms were released from the zeolite framework to form EFAL species. Figure 1b shows the ²⁷Al MAS NMR spectra of the various samples. For nondealuminated zeolites, only one signal at ca. 55 ppm due to four-coordinate framework aluminum was observable. Upon dealumination treatment, another two broad peaks at ca. 30 and 0 ppm due to five- and six-coordinate EFAL species^{22–24} appeared at the expense of the four-coordinate framework aluminum. The ²⁹Si MAS NMR spectra of various samples were shown in Figure 1c. According to the previous work,^{39–42} the simulated Gaussian peaks centering at −100, −106, −112, and −116 ppm in Figure 1c can be tentatively assigned to Si(2Si, 2Al), Si(3Si, 1Al) or Si(3Si, 1SiOH), Si(4Si, 0Al), and Si(4Si, 0Al) units, respectively. By carefully

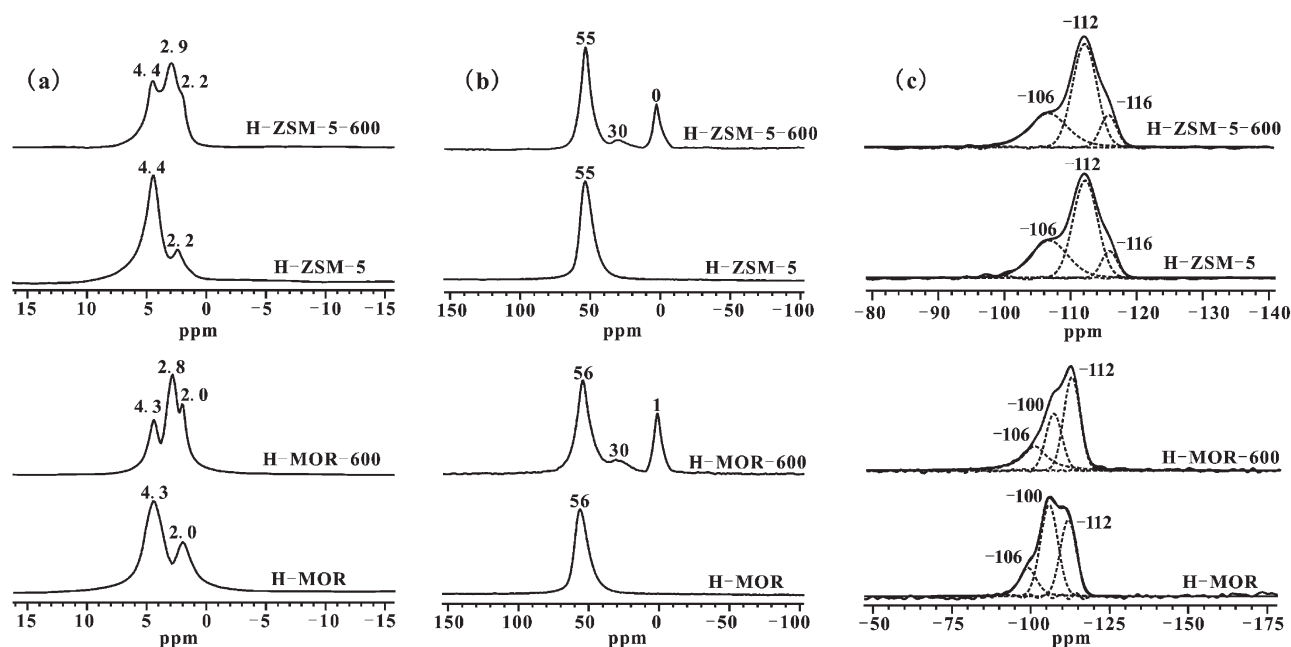


Figure 1. (a) ^1H , (b) ^{27}Al , and (c) ^{29}Si MAS NMR spectra of parent H-ZSM-5, H-ZSM-5-600, parent H-MOR, and H-MOR-600 zeolites.

Table 1. Framework Si/Al Ratios, Relative Integrated Peak Areas of Various Aluminum Species and Hydroxyl Groups in the H-ZSM-5, H-ZSM-5-600, H-MOR, and H-MOR-600 Zeolites

sample	Si/Al ^a	Si/Al ^b	Si/Al ^c	relative peak area (%) ^d			relative peak area (%) ^e		
				Al ^{IV}	Al ^V	Al ^{VI}	SiOHAl	AlOH	SiOH
H-ZSM-5	12.0	12.8		100	0	0	95.8	0	4.2
H-ZSM-5-600	20.8	12.8	19.0	67.4	2.1	30.5	38.5	40.6	20.9
H-MOR	4.8	4.3		100	0	0	94.2	0	5.8
H-MOR-600	8.2	4.5	7.0	64.5	2.3	33.2	35.9	39.3	23.9

^a Si/Al ratios as determined by ^{29}Si MAS NMR. ^b Si/Al ratios as determined by ICP-AES. ^c Si/Al ratios as determined by ICP-AES and ^{27}Al MAS NMR.

^d Relative integrated peak areas of various aluminum species as determined by ^{27}Al MAS NMR. ^e Relative integrated peak areas of various hydroxyl groups as determined by ^1H MAS NMR.

deconvoluting the ^{29}Si NMR MAS spectra of various samples, the framework Si/Al ratios for parent H-ZSM-5 and H-MOR zeolites were determined to be 12.0 and 4.8, respectively, which was comparable to those determined from ICP-AES chemical analysis (see Table 1). In the dealuminated zeolites, more silanol groups associated with Si(3Si, 1SiOH) units will be formed as revealed by ^1H MAS NMR (Figure 1a), and their ^{29}Si chemical shift would overlap with that of Si(3Si, 1Al) groups at around -106 ppm.^{43,44} Thus, the determination of framework Si/Al ratio by ^{29}Si MAS NMR would be less accurate without taking the contribution from silanol groups into account. As shown in Table 1, after taking such a contribution into account, the Si/Al ratio could be estimated to be 20.8 and 8.2 for the dealuminated H-ZSM-5 and H-MOR zeolites, respectively, which is in reasonable agreement with that determined from ICP-AES and ^{27}Al MAS NMR (for details, see the Supporting Information). The results obtained from ^1H , ^{27}Al , and ^{29}Si MAS NMR experiments suggest that calcination treatment leads to dealumination of the parent zeolites.

3.2. ^1H DQ-MAS NMR Experiments. Because the DQ coherences observed are strongly dependent on the internuclear

distance, the presence of a signal in a ^1H DQ-MAS spectrum would indicate that the two protons should be in close proximity; that is, the distance between them is usually less than 5 \AA .³⁰ Peaks that occur along the diagonal (ω , 2ω) are autocorrelation peaks resulting from the dipolar interaction of protons with the same chemical shift, while pairs of off-diagonal peaks at (ω_a , $\omega_a + \omega_b$) and (ω_b , $\omega_a + \omega_b$) correspond to correlations between two protons with different chemical shifts. Figure 2a shows the ^1H DQ-MAS NMR spectrum of parent H-ZSM-5 zeolite. As shown in Figure 2a, only two autocorrelation peaks were observable. The appearance of an autocorrelation peak at (4.4, 8.8) ppm indicates that the bridging hydroxyl groups (SiOHAl, Brønsted acid site) are in close proximity to each other. This means that even in H-ZSM-5 zeolite with a Si/Al of 12.8, the Brønsted acid sites are not isolated but in close proximity. The autocorrelation peak at (2.2, 4.4) ppm corresponds to the spatial proximity between the nonacidic silanols, probably due to the formation of silanol nest during the dealumination process.⁴⁵ Upon dealumination treatment of the zeolite by calcination, notable changes in the ^1H DQ-MAS NMR spectra were observed, as shown in Figure 2b. First, one cross-peak pair at

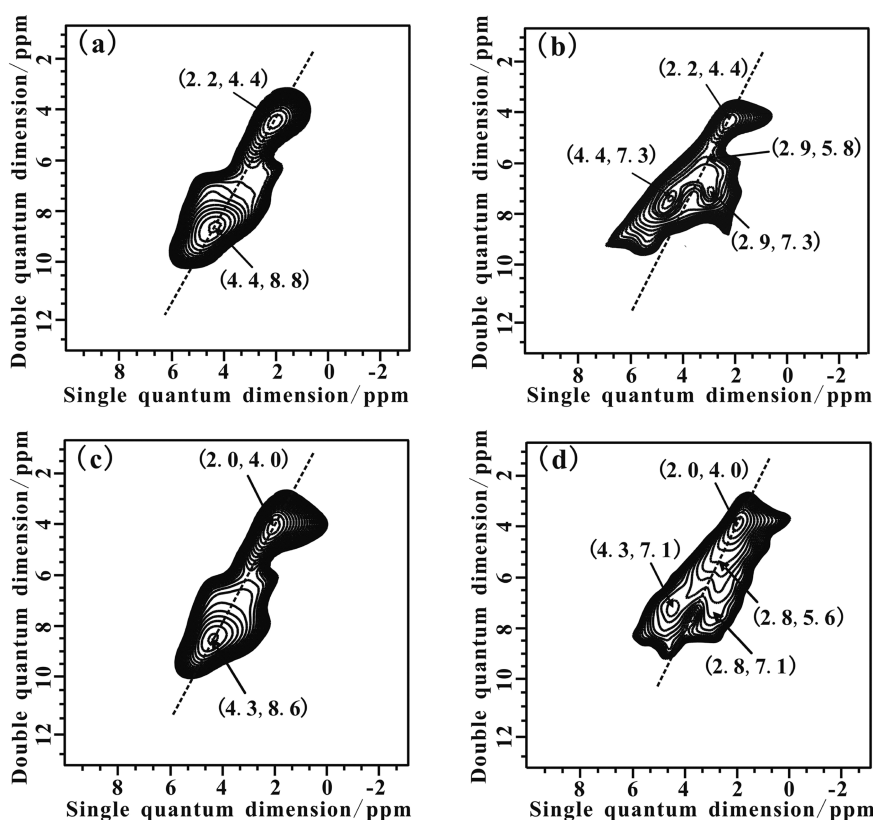


Figure 2. ^1H DQ-MAS NMR spectra of (a) parent H-ZSM-5, (b) H-ZSM-5-600, (c) parent H-MOR, and (d) H-MOR-600 zeolites.

(2.9, 7.3) and (4.4, 7.3) ppm appears, which corresponds to correlations between the adjacent pair of extra-framework AlOH (Lewis acid sites) and the bridging hydroxyl groups (Brønsted acid sites) in the H-ZSM-5-600 zeolite. Second, the autocorrelation peak at (4.4, 8.8) ppm disappears, implying that the Brønsted acid sites are no longer in close proximity but become isolated one another after dealumination. In a previous study, we also found that severe dealumination treatments, such as calcinations of H-Y at 600 and 700 $^{\circ}\text{C}$, could result in the isolation of Brønsted acid sites in both the supercages and the sodalite cages of H-Y zeolite.^{28b} Third, a new autocorrelation peak at (2.9, 5.8) ppm is present, which is due to correlations of hydroxyls in the EFAL species such as $\text{Al}(\text{OH})_3$ or $\text{Al}(\text{OH})_2^+$. For the parent and dealuminated H-MOR samples, their ^1H DQ-MAS NMR spectra (Figure 2c,d) are similar to those of the H-ZSM-5 samples. Therefore, the 2D ^1H DQ-MAS NMR experiment is capable of revealing detailed spatial correlations among various hydroxyl groups in the H-ZSM-5 and H-MOR zeolites. More importantly, the spatial proximities between Brønsted and Lewis acid sites were found in both dealuminated H-ZSM-5 and H-MOR zeolites, implying that the Brønsted/Lewis acid synergy is probably present.

3.3. ^{27}Al DQ-MAS NMR Experiments. To identify the spatial proximity and interaction of various aluminum species in both parent and dealuminated zeolites, a sensitivity-enhanced ^{27}Al DQ-MAS NMR technique³⁶ at high field (18.8 T) was applied to these zeolite samples. Figure 3a shows the ^{27}Al DQ-MAS NMR spectrum of parent H-ZSM-5 zeolite, in which only one autocorrelation peak at (55, 110) ppm is observable. The appearance of the autocorrelation peak at (55, 110) ppm indicates that the four-coordinate framework Al species, which are associated with

bridging hydroxyl groups (SiOHAl , Brønsted acid site), are in close proximity to one another.

Figure 3b shows the ^{27}Al DQ-MAS NMR spectrum of H-ZSM-5-600 zeolite. In comparison with Figure 3a, additional two autocorrelation peaks at (30, 60) and (0, 0) ppm can be clearly distinguished. The appearance of autocorrelation peaks at (30, 60) and (0, 0) ppm indicates that both five- and six-coordinate EFAL species are in close proximity to one another. Apart from the autocorrelation peaks, three distinct cross-peak pairs between (i) four-coordinate framework Al and five-coordinate EFAL ((55, 85), (30, 85) ppm), (ii) four-coordinate framework Al and six-coordinate Al ((55, 55), (0, 55) ppm), and (iii) five-coordinate EFAL and six-coordinate EFAL ((30, 30), (0, 30) ppm) are present, indicating that three kinds of aluminum species are in close proximity to one another. Similar results are also observed for parent H-MOR and H-MOR-600 samples (see Figure 3c and d). It can be concluded from the ^{27}Al DQ-MAS NMR results that the EFAL species (including five- and six-coordinate EFAL) are always in close proximity to the four-coordinate framework aluminum in both dealuminated H-ZSM-5 and dealuminated H-MOR zeolites. Similar phenomenon was previous observed in H-Y zeolite.²⁹ Generally, the four-coordinate framework aluminum is associated with Brønsted acid site (SiOHAl), while EFAL species resulting from the dealumination acts as Lewis acid site in zeolites. Our ^{27}Al DQ-MAS NMR results present here might suggest the existence of Brønsted/Lewis acid synergy from another point of view.

3.4. Variations in the Acid Strength for Dealuminated Zeolites. $2\text{-}^{13}\text{C}$ -Acetone is a well-established NMR probe molecule for measuring the relative Brønsted acid strengths of various solid acids, including zeolites.^{46,47} The formation of a hydrogen

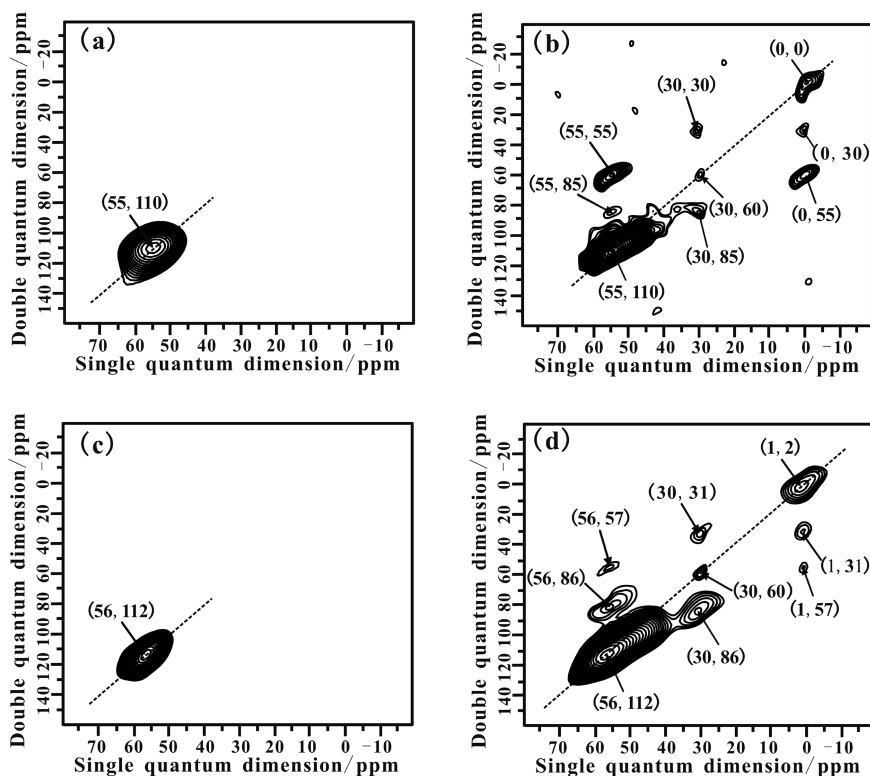


Figure 3. ^{27}Al DQ-MAS NMR spectra of (a) parent H-ZSM-5, (b) H-ZSM-5-600, (c) parent H-MOR, and (d) H-MOR-600 zeolites.

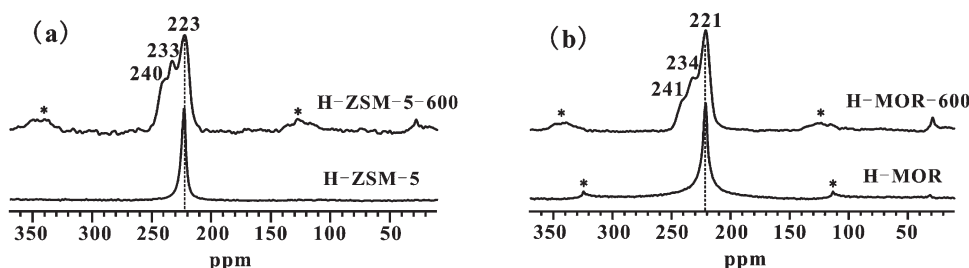


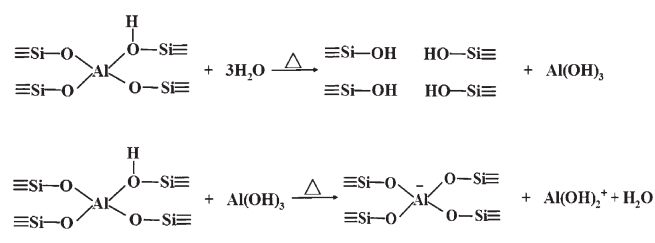
Figure 4. ^{13}C CP/MAS NMR spectra of 2- ^{13}C -acetone adsorbed on (a) parent H-ZSM-5 and H-ZSM-5-600 zeolites, and (b) parent H-MOR and H-MOR-600 zeolites.

bond between the acidic proton and the carbonyl oxygen of adsorbed 2- ^{13}C -acetone will cause a downfield shift of the carbonyl carbon. Generally, the stronger is the Brønsted acidity, the stronger is the hydrogen bonding between the carbonyl carbon and the acidic proton, and consequently the larger is the ^{13}C isotropic chemical shift. Recently, we established a linear correlation between the ^{13}C isotropic chemical shift of adsorbed acetone and Brønsted acid strength with the aid of DFT calculations.⁴⁸ Here, the H-ZSM-5 and H-MOR zeolite samples were further characterized by ^1H - ^{13}C CP/MAS NMR of adsorbed 2- ^{13}C -acetone to identify whether the spatial proximity between Brønsted and Lewis acid sites would result in a synergy effect that enhances the Brønsted acid strength. Figure 4 shows the ^{13}C MAS NMR spectra of 2- ^{13}C -acetone adsorbed on the surface of various samples. For the parent H-ZSM-5 zeolite, as shown in Figure 4a, an intense signal at 223 ppm and a very weak signal at 30 ppm were observable. The former can be assigned to unreacted acetone adsorbed on Brønsted acid sites, while the latter is due to the methyl group of the products of

bimolecular and trimolecular reactions (aldol reaction) of 2- ^{13}C -acetone.^{49–51} For the H-ZSM-5-600 sample, two additional resonance peaks at 233 and 240 ppm can be clearly resolved in the ^{13}C CP/MAS spectrum. The former can be attributed to acetone adsorbed on Brønsted acid sites with a stronger acid strength (as compared to the peak at 223 ppm) that are interacting with Lewis acid sites, whereas the latter is associated with acetone directly adsorbed on Lewis acid sites.²⁸ The larger ^{13}C chemical shift of the 233 ppm signal indicates that the acid strength of the corresponding Brønsted acid site is remarkably enhanced because of the Brønsted/Lewis acid synergy, as compared to the parent H-ZSM-5 zeolite. Similar results were observed for the dealuminated H-MOR zeolite (Figure 4b). Therefore, the ^{13}C NMR results of adsorbed acetone confirm the presence of Brønsted/Lewis acid synergy effect in the dealuminated H-ZSM-5 and H-MOR zeolites.

3.5. Brønsted/Lewis Acid Synergy and Spatial Proximities of Acid Sites. In our previous studies,²⁸ on the basis of ^1H DQ-MAS NMR and DFT calculations, the mechanism of

Scheme 1. Dealumination Mechanism of H-ZSM-5 and H-MOR Zeolites

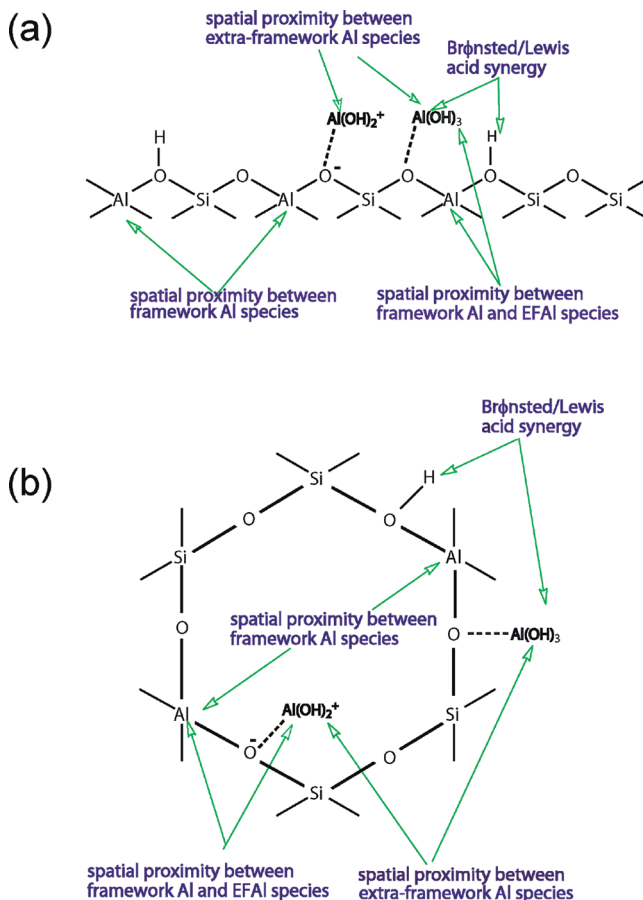


Brønsted/Lewis acid synergy in dealuminated H-Y zeolite was revealed. Moreover, in combination ^{27}Al DQ-MAS NMR with DFT theoretical calculations, it was demonstrated that the dealumination of H-Y zeolite is a successive process.²⁹ In the first step, four-coordinate framework Al is released from zeolite framework, giving rise to six-coordinate $\text{Al}(\text{OH})_3$ EFAL species. In the second step, the $\text{Al}(\text{OH})_3$ EFAL species would interact with the Brønsted acid site (SiOHAl , associated with four-coordinate framework Al), leading to the formation of five-coordinate $\text{Al}(\text{OH})_2^+$ EFAL species by the removal of one water molecule between them. In the third step, the interaction of the $\text{Al}(\text{OH})_2^+$ species with the Brønsted acid site results in the formation of four-coordinate AlOH^{2+} EFAL species by eliminating another one water molecule between them. $\text{Al}(\text{OH})_3$, $\text{Al}(\text{OH})_2^+$, and AlOH^{2+} in the form of six-, five-, and four-coordination, respectively, are the preferred EFAL species in H-Y zeolites dealuminated at different calcination temperatures. Because only the signals of six- and five-coordinate EFAL species were observed, whereas no signal from four-coordinate EFAL species was visible in the ^{27}Al MAS (Figure 1), ^{27}Al DQ-MAS (Figure 3), and ^{27}Al MQ-MAS (not shown) NMR spectra of our H-ZSM-5-600 and H-MOR-600 samples, it can be expected that only the first two dealumination steps occur and the resultant six-coordinate $\text{Al}(\text{OH})_3$ and five-coordinate $\text{Al}(\text{OH})_2^+$ are the preferred EFAL species in the dealuminated H-ZSM-5 and H-MOR zeolites (see Scheme 1).

It is interesting to note that the autocorrelation peak of Brønsted acidic proton disappears in the ^1H DQ-MAS NMR spectra (Figure 2), whereas that of four-coordinate framework aluminum is still present in the ^{27}Al DQ-MAS NMR spectra (Figure 3) of both H-ZSM-5-600 and H-MOR-600 samples. This can be rationalized by the proposed dealumination process (Scheme 1). In the second step, the Brønsted acidic proton and the hydroxyl group of $\text{Al}(\text{OH})_3$ EFAL species are eliminated by forming one water molecule. However, the four-coordinate Al associated with Brønsted acid site is not released but still located in the zeolite framework, which means that much more Brønsted acidic protons are removed during the dealumination process as compared to the four-coordinate framework Al atoms. The negative charge of the framework SiO^-Al unit can be compensated by the positive charge of $\text{Al}(\text{OH})_2^+$ EFAL species.

Although ^{27}Al - ^{27}Al distances cannot be quantitatively obtained from the ^{27}Al DQ-MAS NMR spectra so far, the ^{27}Al DQ experiments were previously tested on some model compounds such as AlPO_4 -14 and AlPO -CJ19 with known crystal structures and ^{27}Al - ^{27}Al distances.^{52,53} It was found that the appearance of ^{27}Al correlation peaks usually suggests that the ^{27}Al - ^{27}Al distance between neighboring aluminum pair is within 6.0 Å. In addition, we also measured the ^1H - ^1H distance between Brønsted acidic protons, which are associated with four-coordinate framework

Scheme 2. Brønsted/Lewis Acid Synergy and Experimentally Observed Spatial Proximities of Various Al Species in Dealuminated H-MOR (a) and Dealuminated H-ZSM-5 (b) Zeolites



Al in parent H-ZSM-5 through ^1H DQ-MAS NMR. The experimentally measured ^1H - ^1H distance is around 4.5 Å (see Figure S1), suggesting that the ^{27}Al - ^{27}Al distance between neighboring framework aluminum pair in H-ZSM-5 zeolite might be around 5.0 Å.

It is noteworthy that as revealed by ^{29}Si MAS NMR, the $\text{Si}(2\text{Al})$ units are present in the H-MOR zeolites and absent in the H-ZSM-5 zeolites. According to the X-ray structure of the two zeolites, the ^{27}Al - ^{27}Al distance of the nearest framework Al pair (associated with $\text{Si}(2\text{Al})$ unit) with four bonds connection ($\text{Al}-\text{O}-\text{Si}-\text{O}-\text{Al}$) in H-MOR zeolite is estimated to be around 4.4–5.3 Å. Obviously, this kind of Al pair can result in the appearance of autocorrelation peaks in the ^{27}Al DQ-MAS spectra of H-MOR zeolites. For the H-ZSM-5 zeolite, the absence of $\text{Si}(2\text{Al})$ units implies the absence of the nearest framework Al pair. Therefore, the existence of the next nearest framework Al pair with six bonds connection ($\text{Al}-\text{O}-\text{Si}-\text{O}-\text{Si}-\text{O}-\text{Al}$) is possible. If such a connection is located in the 10-membered ring of H-ZSM-5 zeolite, the ^{27}Al - ^{27}Al distance is around 6.8–8.4 Å. If such a connection is present in the six-membered ring (some of the six-membered rings are facing the 10-membered rings), the ^{27}Al - ^{27}Al distance is roughly estimated to be around 4.7–5.6 Å. If such a connection exists in the four- or five-membered ring, the $\text{Si}(2\text{Al})$ unit will be formed. Therefore, the existence of the next nearest framework Al pair in

the six-membered ring of H–ZSM-5 zeolite can solely satisfy the condition to generate the autocorrelation peaks in the ^{27}Al DQ-MAS NMR spectra of H–ZSM-5 zeolites. Because the framework Al is associated with the Brønsted acid site (SiOHAl), such an Al pair is also able to result in the appearance of autocorrelation peak in the ^1H DQ-MAS NMR spectrum of parent H–ZSM-5 zeolite (see Figure 2a).

On the basis of our previous studies^{28,29} and the present experimental results, it can be concluded that the Brønsted/Lewis acid synergy is probably a common phenomenon present in various dealuminated zeolites, including H–Y, H–ZSM-5, and H–MOR zeolites. The synergy mechanism and the experimentally observed spatial proximities of various Al species are illustrated in Scheme 2a for dealuminated H–MOR in Scheme 2b for dealuminated H–ZSM-5. The coordination of Lewis acid site ($\text{Al}(\text{OH})_3$) to the oxygen atom nearest to Brønsted acid site may cause a partial electron transfer from the OH bond of the acid site to the $\text{Al}(\text{OH})_3$ species, which would increase the acid strength of the site by decreasing the OH bond strength. The synergetic effect of the $\text{Al}(\text{OH})_2^+$ EFAL species on the adjacent Brønsted acid site might be negligible due to the relatively long distance between them. It should be noted that, based on our ^1H DQ-MAS NMR experiments, the Brønsted/Lewis acid synergy illustrated in scheme 2b is also likely present in the 10-membered ring of H–ZSM-5 zeolite.

4. CONCLUSION

The Brønsted/Lewis acid synergy and spatial proximities of acid sites in H–ZSM-5 and H–MOR zeolites were investigated by ^1H and ^{27}Al DQ-MAS NMR techniques in conjunction with ^{13}C CP/MAS NMR of adsorbed 2- ^{13}C -acetone. Both ^1H and ^{27}Al DQ-MAS NMR results revealed that Lewis acid sites are in close proximity to Brønsted acid sites, implying the existence of Brønsted/Lewis acid synergy in dealuminated H–ZSM-5 and H–MOR zeolites. The ^{13}C CP/MAS NMR of adsorbed 2- ^{13}C -acetone confirmed a remarkable increase in the acid strength of the dealuminated zeolites due to the existence of Brønsted/Lewis acid synergy. In addition, the ^{27}Al DQ-MAS NMR also demonstrated that six-coordinate $\text{Al}(\text{OH})_3$ and five-coordinate $\text{Al}(\text{OH})_2^+$ are the preferred EFAL species and are in close proximity to four-coordinate framework Al species in the dealuminated zeolites. The results present here might be helpful for studying the mechanism of various acid-catalyzed reactions occurring over dealuminated H–ZSM-5 and H–MOR zeolites and for modifying related catalysts for specified applications.

■ ASSOCIATED CONTENT

S Supporting Information. Si/Al ratio calculations for dealuminated zeolites and ^1H – ^1H distance measurement from ^1H DQ-MAS NMR experiments. This material is available free of charge via the Internet at <http://pubs.acs.org>.

■ AUTHOR INFORMATION

Corresponding Author

*Fax: +86-27-87199291. E-mail: dengf@wipm.ac.cn.

Author Contributions

[§]These authors contributed equally to the work

■ ACKNOWLEDGMENT

This work was supported by the National Natural Science Foundation of China (21003154, 20933009, and 20921004), the Ministry of Science of Technology of China (2009IM-03700), and the National Basic Research Program of China (2009CB918600).

■ REFERENCES

- (1) Weisz, P. B. *Pure Appl. Chem.* **1980**, *58*, 841.
- (2) Campbell, S. M.; Bibby, D. M.; Coddington, J. M.; Howe, R. F.; Meinhold, R. H. *J. Catal.* **1996**, *161*, 350.
- (3) Sun, X. D.; Wang, Q. X.; Xu, L. Y.; Liu, S. L. *Catal. Lett.* **2004**, *94*, 75.
- (4) Feller, A.; Guzman, A.; Zuazo, I.; Lercher, J. A. *J. Catal.* **2004**, *224*, 80.
- (5) Smit, B.; Maesen, T. L. M. *Nature* **2008**, *451*, 671.
- (6) Huang, J.; Jiang, Y. J.; Marthala, V. R. R.; Hunger, M. *J. Am. Chem. Soc.* **2008**, *130*, 12642.
- (7) (a) Mota, C. J. A.; Bhering, D. L.; Rosenbach, N. *Angew. Chem., Int. Ed.* **2004**, *43*, 3050. (b) Carvajal, R.; Chu, P.; Lunsford, J. H. *J. Catal.* **1990**, *125*, 123.
- (8) (a) Sokol, A. A.; Catlow, C. R. A.; Garces, J. M.; Kuperman, A. *Adv. Mater.* **2000**, *12*, 1801. (b) van Bokhoven, J. A.; van der Eerden, A. M. J.; Koningsberger, D. C. *J. Am. Chem. Soc.* **2003**, *125*, 7435.
- (9) DeCanio, S. J.; Sohn, J. R.; Fritz, P. O.; Lunsford, J. H. *J. Catal.* **1986**, *101*, 132.
- (10) Sohn, J. R.; DeCanio, S. J.; Fritz, P. O.; Lunsford, J. H. *J. Phys. Chem.* **1986**, *90*, 4847.
- (11) Beyerlein, R. A.; McVicker, G. B.; Yacullo, L. N.; Ziemiak, J. *J. Phys. Chem.* **1988**, *92*, 1967.
- (12) Corma, A.; Fornes, V.; Rey, F. *Appl. Catal.* **1990**, *59*, 267.
- (13) Lonyi, F.; Lunsford, J. H. *J. Catal.* **1992**, *136*, 566.
- (14) Batamack, P.; Morin, C. D.; Vincent, R.; Fraissard, J. *Micro-porous Mesoporous Mater.* **1994**, *2*, 525.
- (15) Viswanadham, N.; Gupta, J. K.; Dhar, G. M.; Garg, M. O. *Energy Fuels* **2006**, *20*, 1806.
- (16) Kanellopoulos, J.; Unger, A.; Schwiager, W.; Freude, D. *J. Catal.* **2006**, *237*, 416.
- (17) Mirodatos, C.; Barthomeuf, D. *J. Chem. Soc., Chem. Commun.* **1981**, 39.
- (18) Hunger, M. *Catal. Rev.-Sci. Eng.* **1997**, *39*, 345.
- (19) Freude, D.; Kärger, J.; Schüth, F. In *Handbook of Porous Materials*; Sing, K.; Weitkamp, J., Eds.; Wiley-VCH: Chichester, 2002; Vol. 1, p 465.
- (20) Hunger, M. *Solid State Nucl. Magn. Reson.* **1996**, *6*, 1.
- (21) (a) Mildner, T.; Freude, D. *J. Catal.* **1998**, *178*, 309. (b) Huo, H.; Peng, L. M.; Grey, C. P. *J. Phys. Chem. C* **2009**, *113*, 8211.
- (22) Fyfe, C. A.; Bretherton, J. L.; Lam, L. Y. *J. Am. Chem. Soc.* **2001**, *123*, 5285.
- (23) Jiao, J.; Kanellopoulos, J.; Wang, W.; Ray, S. S.; Foerster, H.; Freude, D.; Hunger, M. *Phys. Chem. Chem. Phys.* **2005**, *7*, 3221.
- (24) van Bokhoven, J. A.; Koningsberger, D. C.; Kunkeler, P.; van Bekkum, H.; Kentgens, A. P. M. *J. Am. Chem. Soc.* **2000**, *122*, 12842.
- (25) Haw, J. F.; Nicholas, J. B.; Xu, T.; Beck, L. W.; Ferguson, D. B. *Acc. Chem. Res.* **1996**, *29*, 259.
- (26) Rothwell, W. P.; Shen, W.; Lunsford, J. H. *J. Am. Chem. Soc.* **1984**, *106*, 2452.
- (27) Huang, J.; Jiang, Y. J.; Marthala, V. R. R.; Thomas, B.; Romanova, E.; Hunger, M. *J. Phys. Chem. C* **2008**, *112*, 3811.
- (28) (a) Li, S. H.; Zheng, A. M.; Su, Y. C.; Zhang, H. L.; Chen, L.; Yang, J.; Ye, C. H.; Deng, F. *J. Am. Chem. Soc.* **2007**, *129*, 11161. (b) Li, S. H.; Huang, S. J.; Shen, W. L.; Zhang, H. L.; Fang, H. J.; Zheng, A. M.; Liu, S. B.; Deng, F. *J. Phys. Chem. C* **2008**, *112*, 14486. (c) Li, S. H.; Zheng, A. M.; Su, Y. C.; Fang, H. J.; Shen, W. L.; Yu, Z. W.; Chen, L.; Deng, F. *Phys. Chem. Chem. Phys.* **2010**, *12*, 3895.
- (29) Yu, Z. W.; Zheng, A. M.; Wang, Q.; Chen, L.; Xu, J.; Amoureux, J. P.; Deng, F. *Angew. Chem., Int. Ed.* **2010**, *49*, 8657.

- (30) Brown, S. P.; Spiess, H. W. *Chem. Rev.* **2001**, *101*, 4125.
- (31) (a) Brouwer, D. H.; Darton, R. J.; Morris, R. E.; Levitt, M. H. *J. Am. Chem. Soc.* **2005**, *127*, 10365. (b) Brouwer, D. H.; Kristiansen, P. E.; Fyfe, C. A.; Levitt, M. H. *J. Am. Chem. Soc.* **2005**, *127*, 542.
- (32) Edén, M.; Zhou, D.; Yu, J. H. *Chem. Phys. Lett.* **2006**, *431*, 39.
- (33) Malicki, N.; Mali, G.; Quoineaud, A. A.; Bourges, P.; Simon, L. J.; Thibault-Starzyk, F.; Fernandez, C. *Microporous Mesoporous Mater.* **2010**, *129*, 100.
- (34) Hohwy, M.; Jakobsen, H. J.; Eden, M.; Levitt, M. H.; Nielsen, N. C. *J. Chem. Phys.* **1998**, *108*, 2686.
- (35) Madhu, P. K.; Goldbourt, A.; Frydman, L.; Vega, S. *Chem. Phys. Lett.* **1999**, *307*, 41.
- (36) Wang, Q.; Hu, B.; Lafon, O.; Trébosc, J.; Deng, F.; Amoureux, J. P. *J. Magn. Reson.* **2009**, *200*, 251.
- (37) Deng, F.; Yue, Y.; Ye, C. H. *Solid State Nucl. Magn. Reson.* **1998**, *10*, 151.
- (38) (a) Beck, L. W.; Haw, J. F. *J. Phys. Chem.* **1995**, *99*, 1076. (b) Gabrienko, A. A.; Danilova, I. G.; Arzumanov, S. S.; Toktarev, A. V.; Freude, D.; Stepanov, A. G. *Microporous Mesoporous Mater.* **2010**, *131*, 210.
- (39) Barras, J.; Klinowski, J.; McComb, D. W. *J. Chem. Soc., Faraday Trans.* **1994**, *90*, 3719.
- (40) Sano, T.; Wakabayashi, S.; Oumi, Y.; Uozumi, T. *Microporous Mesoporous Mater.* **2001**, *46*, 67.
- (41) Dedeczek, J.; Sklenak, S.; Li, C.; Wichterlova, B.; Gabova, V.; Brus, J.; Sierka, M.; Sauer, J. *J. Phys. Chem. C* **2009**, *113*, 1447.
- (42) Hayashi, S.; Kojima, N. *Microporous Mesoporous Mater.* **2011**, *141*, 49.
- (43) Zhang, W. P.; Bao, X. H.; Guo, X. W.; Wang, X. S. *Catal. Lett.* **1999**, *60*, 89.
- (44) Campbell, S. M.; Bibby, D. M.; Coddington, J. M.; Howe, R. F.; Meinhold, R. H. *J. Catal.* **1996**, *161*, 338.
- (45) Wang, Q. L.; Giannetto, G.; Guisnet, M. *J. Catal.* **1991**, *130*, 471.
- (46) Xu, M. C.; Arnold, A.; Buchholz, A.; Wang, W.; Hunger, M. *J. Phys. Chem. B* **2002**, *106*, 12140.
- (47) Biaglow, A. I.; Gorte, R. J.; Kokotailo, G. T.; White, D. *J. Catal.* **1994**, *148*, 779.
- (48) Fang, H. J.; Zheng, A. M.; Chu, Y. Y.; Deng, F. *J. Phys. Chem. C* **2010**, *114*, 12711.
- (49) Xu, T.; Kob, N.; Drago, R. S.; Nicholas, J. B.; Haw, J. F. *J. Am. Chem. Soc.* **1997**, *119*, 12231.
- (50) Xu, T.; Haw, J. F. *J. Am. Chem. Soc.* **1994**, *116*, 10188.
- (51) Biaglow, A. I.; Sepa, J.; Gorte, R. J.; White, D. *J. Catal.* **1995**, *151*, 373.
- (52) Mali, G.; Taulelle, F. *Chem. Commun.* **2004**, 868.
- (53) Mali, G.; Fink, G.; Taulelle, F. *J. Chem. Phys.* **2004**, *120*, 2835.